



HAL
open science

Comparison of low, medium and high fidelity numerical methods for unsteady aerodynamics and nonlinear aeroelasticity

Claudia Fernandez-Escudero, Miguel Gagnon, Eric Laurendeau, Sébastien Prothin, Guilhem Michon, Annie Ross

► To cite this version:

Claudia Fernandez-Escudero, Miguel Gagnon, Eric Laurendeau, Sébastien Prothin, Guilhem Michon, et al.. Comparison of low, medium and high fidelity numerical methods for unsteady aerodynamics and nonlinear aeroelasticity. IUTAM Symposium on Critical flow dynamics involving moving/deformable structures with design applications, Jun 2018, Santorini, Greece. pp.0. hal-03487289v1

HAL Id: hal-03487289

<https://hal.science/hal-03487289v1>

Submitted on 30 May 2023 (v1), last revised 20 Jul 2022 (v2)

HAL is a multi-disciplinary open access archive for the deposit and dissemination of scientific research documents, whether they are published or not. The documents may come from teaching and research institutions in France or abroad, or from public or private research centers.

L'archive ouverte pluridisciplinaire **HAL**, est destinée au dépôt et à la diffusion de documents scientifiques de niveau recherche, publiés ou non, émanant des établissements d'enseignement et de recherche français ou étrangers, des laboratoires publics ou privés.

Comparison of low, medium and high fidelity numerical methods for unsteady aerodynamics and nonlinear aeroelasticity.

Claudia FERNANDEZ ESCUDERO ⁽¹⁾, Miguel GAGNON ⁽²⁾,
Eric LAURENDEAU ⁽²⁾, Sebastien PROTHIN ⁽³⁾, Guilhem MICHON ⁽⁴⁾,
Annie ROSS ⁽²⁾.

⁽¹⁾ ISAE-Supaero, Toulouse, France/ Polytechnique Montreal, Canada
(Claudia.FERNANDEZ-ESCUDERO@isae-supaeero.fr).

⁽²⁾ Polytechnique Montreal, Canada.

⁽³⁾ ISAE-Supaero, Toulouse, France.

⁽⁴⁾ Universite de Toulouse, ICA, CNRS, ISAE-Supaero, Toulouse, France.

Abstract. The unsteady aerodynamic and aeroelastic behaviour of a 2D wing section with and without flap is analysed with Unsteady Vortex Lattice Method and Theodorsen theory (low fidelity), Euler (medium fidelity) and Reynolds-Averaged Navier Stokes (high fidelity) methods. The aeroelastic study is carried out both for linear cases and for non-linear structural configurations presenting cubic stiffness and freeplay. The critical flutter speed as well as the limit cycle oscillations present in the non-linear cases are compared. The methods showed good agreement in capturing unsteady aerodynamics and linear and non-linear aeroelasticity for the cases studied.

Key words: Aeroelasticity, Unsteady Aerodynamics, Flutter, LCO, Non-linear, Theodorsen, Vortex Lattice Method, Reynolds Averaged, Navier Stokes, Euler, Control Surface, Freeplay, Cubic Stiffness.

1. Introduction

Aeroelasticity, the study of the coupling between a flexible body and aeroelastic forces, remains today a subject of great interest in aircraft design. It includes the study of static aeroelastic effects and the analysis of more complex problems which appear when dynamic systems are considered. Moreover, aeroelasticity is often affected by non-linearities which alter the system's response; it is the subject of active research[1]. These non-linearities have two different sources: structural elements such as freeplay or cubic stiffness [2] can appear alone or simultaneously in any of the degrees of freedom (DOF) of the airfoil [3] and aerodynamic effects which are mainly due to either transonic effects [4] or to dynamic flow separation due to large deflections in wings, known as stall flutter [3]. The present paper focuses on the two structural non-linearities mentioned, i.e. freeplay and cubic stiffness.

An important phenomenon encountered in dynamic aeroelasticity is flutter. If there are no sources of non-linearities the system can only experience classic flutter which is defined as self-excited vibration of the structure due to energy extraction of the incident airflow. This generally results from the coalescence of two structural modes: pitch and plunge, which reach the same vibration frequency. If the speed becomes greater than the flutter speed, the amplitude of the movement grows exponentially causing structural failure [5].

The presence of non-linearities can change dramatically the observed behaviour as other phenomena, such as limit cycle oscillations (LCOs), can appear in the system's response. During a LCO, the vibration reaches a stable amplitude which remains constant unless the wind speed changes. LCOs can be observed in subcritical or in supercritical regime once flutter speed is passed [4]. It has been found that when non-linearities govern the system's behaviour, initial conditions may cause the system's response to change between two or more possible stable outcomes [6].

The aim of this work is to compare the ability of different numerical methods to capture unstable aerodynamics and aeroelastic behaviour. The aerodynamic forces acting on the airfoil are computed and these forces together with the equations of motion enable the computation of the fluid-structure effects and therefore the resolution of the aeroelastic system. For the aeroelastic analysis, both the linear and the non-linear cases are studied. In the non-linear 2DOF case, cubic stiffness and freeplay gap are applied in the pitch restoring force whereas only freeplay in the control surface deflection is applied in the 3DOF case. The work carried out by Luc Amar in his PhD Thesis [7] is continued with the updated codes now available in our lab, i.e. the new version of UVLM and the use of NLFD (Non-Linear Frequency Domain) for the high fidelity solvers.

2. Structural Model

Two configurations are tested regarding the 2D typical wing section: a 2DOF and a 3DOF airfoil. The 2DOF are heave h and pitch α and the 3DOF case refers to an airfoil with an added control surface that can rotate around its elastic axis β . The airfoil chosen is a NACA0012. *Figure 1* presents the degrees of freedom for each case and the main geometrical parameters: b is the semi chord length, ab and cb are the midchord to elastic axis of the profile and of the control surface distance respectively and $x_\alpha b$ and $x_\beta b$ are the centre of gravity to elastic axis distance of the airfoil and of the control surface respectively.

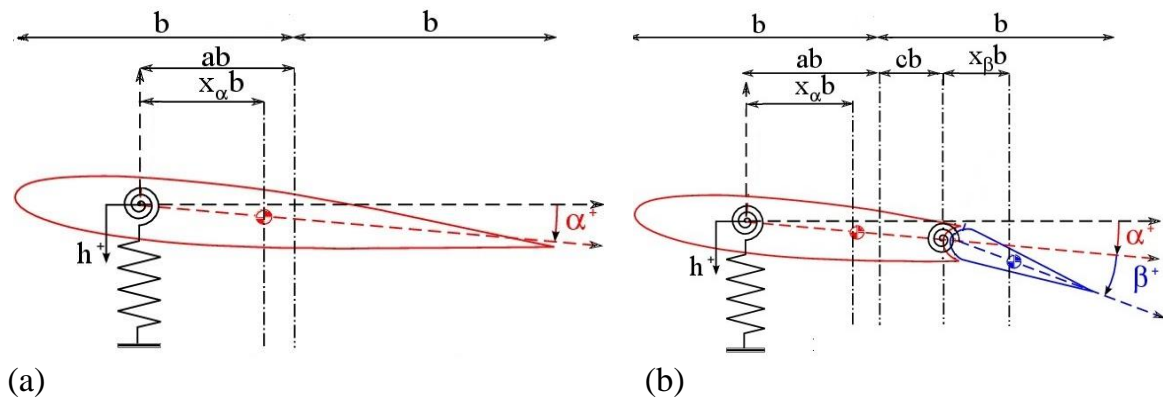


Figure 1. (a) 2DOF and (b) 3DOF typical aeroelastic sections. [7]

The dimensionless aeroelastic equation of motion of an airfoil is:

$$M_s \ddot{q} + B_s \dot{q} + (1 - \nu) K_s q + \nu f_s(q) = f_a(t) \quad (1)$$

M_s , B_s and K_s represent respectively the inertial, damping and stiffness matrices, q is a vector containing the degrees of freedom such that: $q = [h, \alpha, \beta]^T$ and f_s and f_a are vectors containing respectively the restoring and aerodynamic forces. ν is a switch parameter which has a value of either 1 when the system is non-linear and 0 when the system is linear.

In order to solve the fluid structure interaction, f_a will be computed at a given time step and the effect on the structure in terms of position and velocity and acceleration will be calculated. These values of the structure will affect the computation of f_a in the following time step and so on.

Non-linearities are introduced in the pitch restoring force in the form of a cubic stiffness and a freeplay gap in the 2DOF case [8] (*see Figure 2*). In the 3DOF case, freeplay is introduced in control surface deflection [9]:

$$f_{s,\alpha} = \begin{cases} r_\alpha^2 \sum_{k=1}^n \eta_{\alpha,k} (\alpha - \alpha_s)^k, & \text{if } \alpha > \alpha_s \\ r_\alpha^2 \sum_{k=1}^n \eta_{\alpha,k} (\alpha + \alpha_s)^k, & \text{if } \alpha < -\alpha_s \\ 0, & \text{else} \end{cases} \quad (2)$$

$$f_{s,\beta} = \begin{cases} r_\beta^2 \sum_{k=1}^n \Omega_{\beta,k}^2 (\beta - \beta_s)^k, & \text{if } \beta > \beta_s \\ r_\beta^2 \sum_{k=1}^n \Omega_{\beta,k}^2 (\beta + \beta_s)^k, & \text{if } \beta < -\beta_s \\ 0, & \text{else} \end{cases} \quad (3)$$

where α_s and β_s are half of the freeplay gap angle in pitch and in control surface deflection, r_α and r_β are the reduced radius of gyration defined as $r_{\alpha/\beta} = \sqrt{\frac{I_{\alpha/\beta}}{mb^2}}$ where m is the mass of the airfoil and $I_{\alpha/\beta}$ are the structural inertias, $\eta_{\alpha,k}$ is the ratio between the k^{th} non-linear quadratic stiffness and the linear stiffness and $\Omega_{\beta,k}$ is the reduced uncoupled natural frequency at the k^{th} order.

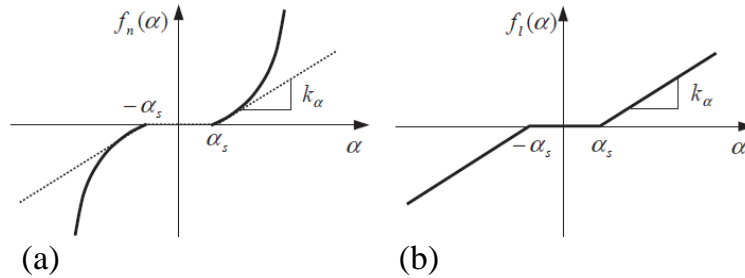


Figure 2. Non-linear pitch stiffness: (a) cubic stiffness with freeplay; (b) freeplay. [8]

3. Aerodynamic Models

Different numerical approaches are used to model the aerodynamic forces vector, f_a . In this work, the aerodynamic is considered as linear.

The Theodorsen approach assumes harmonic motion and is valid for thin profiles with small deflections immersed in linear incompressible and irrotational flows. Its ability to capture LCOs in non-linear cases was demonstrated [9]. Contrary to the quasi-stationary force approach, Theodorsen takes into account the effects of the wake on the profile by imposing the impermeability and the Kutta conditions. The vortices shed are assumed to be aligned with the profile resulting in a flat wake. The original formulation is in frequency domain [10] and remains convenient as long as the system is linear. However, for non-linear cases the equations are more easily solved in the time domain and the Jones approximation is used [11].

In the Unsteady Vortex Lattice Method (UVLM), the airfoil and the aileron are discretised into panels and the transport of vortices is accounted for by a shedding wake [12]. Each panel contains a vortex at $\frac{1}{4}$ of its length and a collocation point at $\frac{3}{4}$ of the length (*see figure 3*). The vortex points induce a velocity on the rest of the panels and their influence is calculated in the collocation points. The Kutta condition is satisfied by imposing the same vorticity on the shed wake and on the trailing edge panel. The Neumann boundary condition on the airfoil closes the system [12]. Some limitations remain, as the thin airfoil and potential flow hypothesis still apply.

The structure of the UVLM code is fully described in [12]. The algorithm obtains the vorticity at each point (γ) by solving a linear system of equations:

$$\text{AIC} * \gamma = \text{RHS} \quad (4)$$

where AIC is the Aerodynamic Influence Coefficients matrix which contains the induced velocities ($v_{j,i}$) calculated as:

$$v_{j,i} = \frac{\gamma_j}{2\pi r_{ij}^2} \begin{Bmatrix} y_i - y_j \\ x_i - x_j \end{Bmatrix} \quad (5)$$

RHS is a vector containing the reduced inflow velocity, the reduced airfoil velocity and the position of the airfoil.

Once the vorticities are obtained, the pressure coefficient is calculated using the unsteady Bernoulli equation:

$$C_{p,i} = \frac{\gamma_{i,k}}{\Delta t} * (u_\infty - v_{m,i} + \sum_{l=1}^k v_{l,i}) * n_i + \frac{1}{\Delta t} \sum_{m=1}^i \gamma_{i,k} - \gamma_{i,k-1} \quad (6)$$

which enables the calculation of the rest of the aerodynamic coefficients.

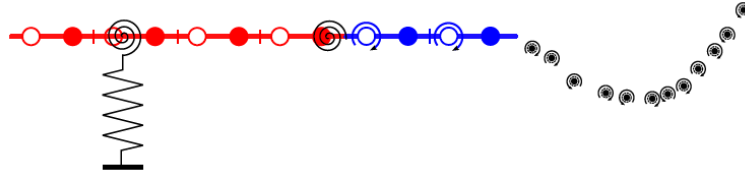


Figure 3. UVLM airfoil discretisation schema. [8]

Euler and Unsteady Reynolds-Averaged Navier Stokes (URANS) solvers compute the aerodynamic forces by discretising space into a mesh, the difference being that only the URANS equations account for viscosity effects through the use of a turbulence model. The aerodynamic solvers used are NSCODE [13]. In this case the Spalart-Allmaras turbulence model [14] is used. NSCODE uses multigrid, artificial dissipation and an implicit LUSGS (Lower-Upper Symmetric Gauss-Seidel) solver scheme. Different meshes and different time steps have been tested in order to capture the aerodynamic behaviour with precision. O-meshes with 129x129, 257x257 and 513x513 meshes were used and the results of the intermediate mesh (257x257) are given. Euler model has been solved with both DTS (Dual-Time Stepping) [15] and NLFD (Non-Linear Frequency Domain) methods [16]. For DTS, there were 500 time steps per period, the simulations were carried out for 7 complete periods and a convergence analysis was performed with 1000 time steps per period. Regarding NLFD, convergence analysis was carried out with 3, 5 and 6 modes and the results shown correspond to the 3 mode analysis.

Table 1 presents approximate computation time for each of the methods presented. Regarding aeroelastic simulations, the aerodynamic force calculation is what determines the total computation time since the time taken for the structural equation resolution is comparatively negligible.

Method	Computation Time on Intel 3930K CPU
Theodorsen	~1 ms/time step
UVLM	~100 ms/iteration
Euler DTS	~300ms/iteration
Euler NLFD (all modes)	~5 min. convergence 10^{-6}
URANS NLFD (all modes)	~15 min. convergence 10^{-6}

Table 1. Approximate computation time for each method.

4. Unsteady aerodynamics

In order to validate the potential aerodynamic models as a preliminary step prior to including structural analysis for aeroelasticity, imposed plunge and pitch motions of the 2DOF airfoil are simulated (*Figures 4 and 5*). The cases chosen are those presented in Yang [15] and in Conner [9] respectively. In this section, only the aerodynamic forces are considered and not the structure's response to these forces.

For each case, the Mach (M) and Reynolds (Re) numbers are given showing that the tests are in low subsonic regime, where the incompressibility hypothesis is reasonable. The imposed vibration frequency is characterised by the dimensionless value known as reduced frequency $K = \frac{\omega c}{2U_\infty}$ where ω is the oscillating frequency (in rad/s), c is the airfoil chord and U_∞ is the incident flow speed. The dimensionless amplitude of the movement is given by h/b in the plunge case. In the pitch case, the airfoil moves around a position referred to as "mean alpha" with amplitude alpha. The low-fidelity methods agrees in capturing the aerodynamic coefficient Cl at moderate reduced frequency and small oscillations (*Figures 2 and 3*). *Table 2* shows the aerodynamic coefficients obtained for a motionless profile at 4.93° angle of attack by the different methods.

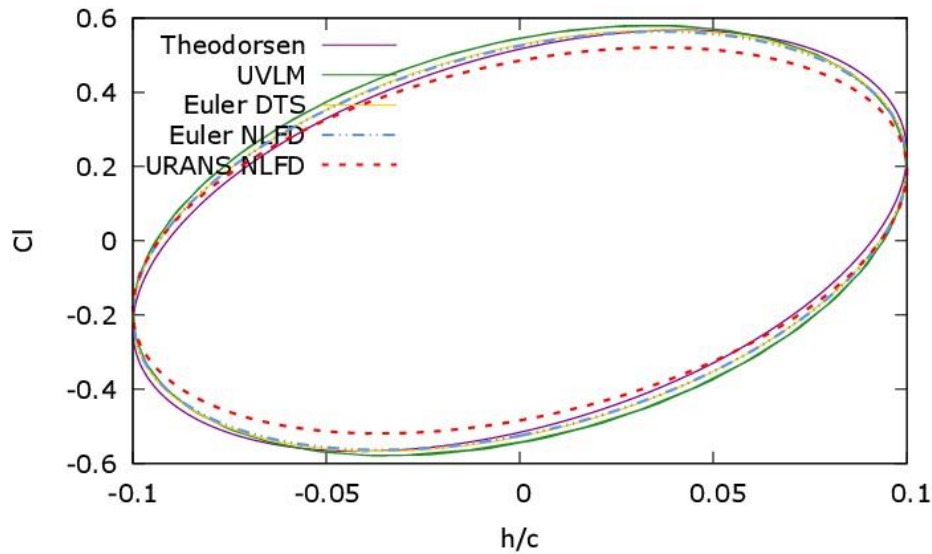


Figure 4. Plunge motion. $M=0.1$, $Re= 1.18M$, $K=0.75$, $h/b=0.1$

	Theodorsen	UVLM	Euler	URANS
Cl	0.54	0.54	0.63	0.57

Table 2. Steady aerodynamic coefficient. $M =0.301$, $Re=3.91M$, $K=0$, Mean alpha= 4.93°

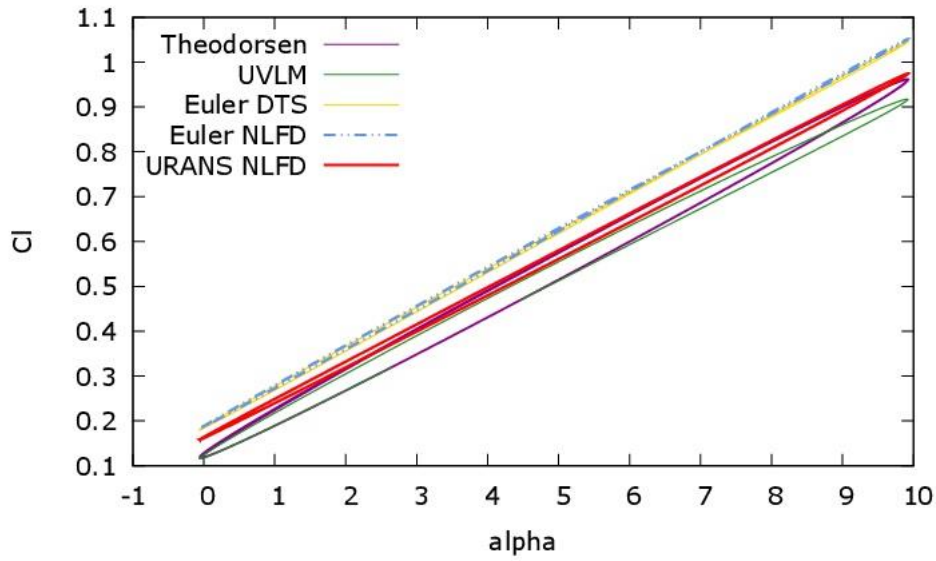


Figure 5. Pitch motion. $M=0.301$, $Re=3.91M$, $K=0.198$, $\alpha=4.99^\circ$, Mean $\alpha=4.93^\circ$

5. Linear Aeroelasticity

In order to carry out flutter analysis, the dimensionless aeroelastic equation of motion of the airfoil (*equation 1*) is computed using the aerodynamic force calculated with the numerical methods already presented. The cases tested are those presented in [8] and in [9] for the 2DOF and 3DOF cases respectively, where the parameters have the values presented in *table 3*. The structural parameters already shown are present, as well as $k = \frac{\rho\pi b^2}{m}$ which is called the mass ratio, and ζ_h , ζ_α and ζ_β , are the structural damping ratio for each DOF. For UVLM, a Fast Fourier Transform (FFT) was applied to go from time domain to frequency domain. The natural frequencies of each DOF are represented by ω_h , ω_α and ω_β .

	2DOF	3DOF
k	1/100	0.03984
a	-0.5	-0.5
c	n/a	0.5
x_α	0.25	0.434
x_β	n/a	0.01996
r_α	0.5	0.7321
r_β	n/a	0.11397
ω_h/ω_α	0.2	0.8078
$\omega_\beta/\omega_\alpha$	n/a	2.0746
ζ_α	0	0.01626
ζ_h	0	0.0115
ζ_β	n/a	0.0113
β_s	0.5°	2.12
$\eta_{\alpha,k}$	3	0

Table 3. Values of parameters for flutter prediction cases.

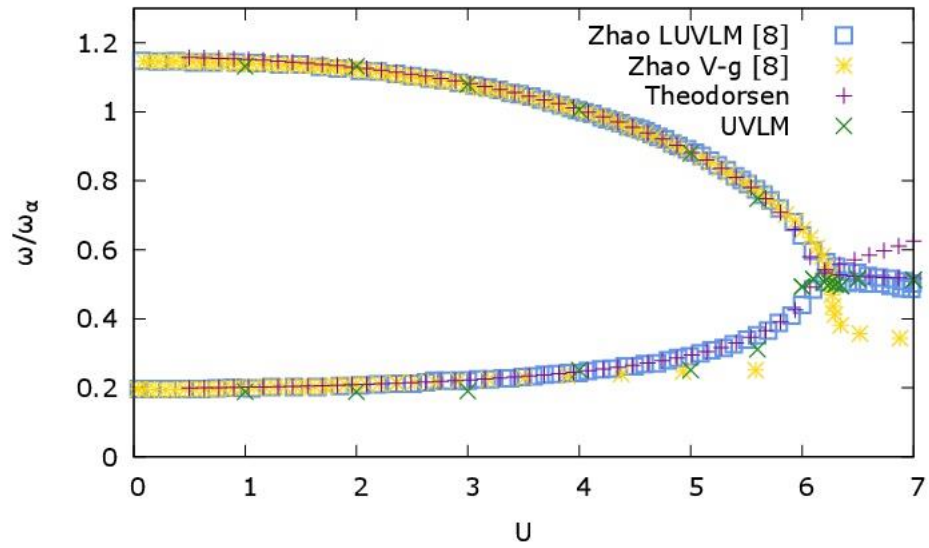


Figure 6. Dimensionless oscillation frequency against dimensionless wind speed for 2DOF linear case.

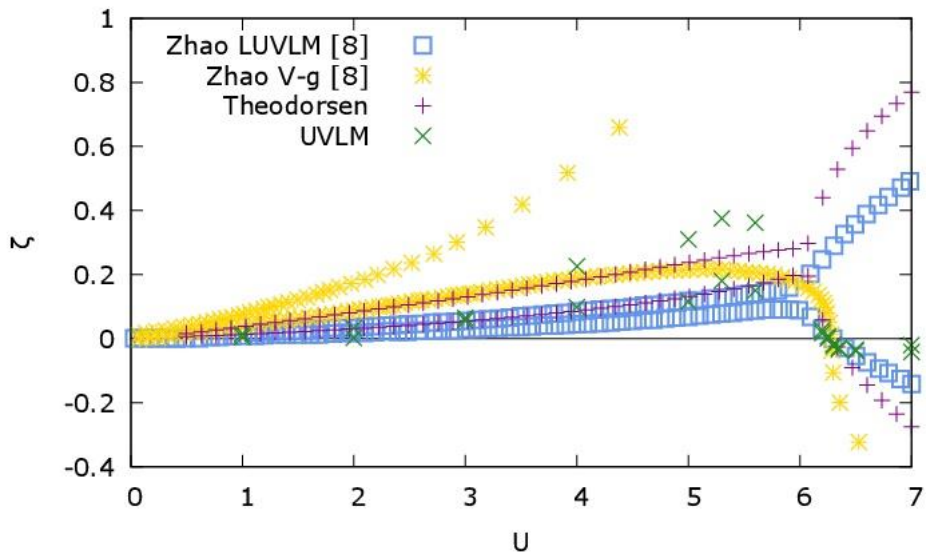


Figure 7. Damping against dimensionless wind speed for the 2DOF linear case.

	Theodorsen	UVLM	Zhao V-g	Zhao LUVLM
U_f	6.29	6.27	6.29	6.29

Table 4. Comparison of dimensionless flutter velocities for the 2DOF linear case.

COMPARISON OF NUMERICAL METHODS FOR AEROELASTICITY.

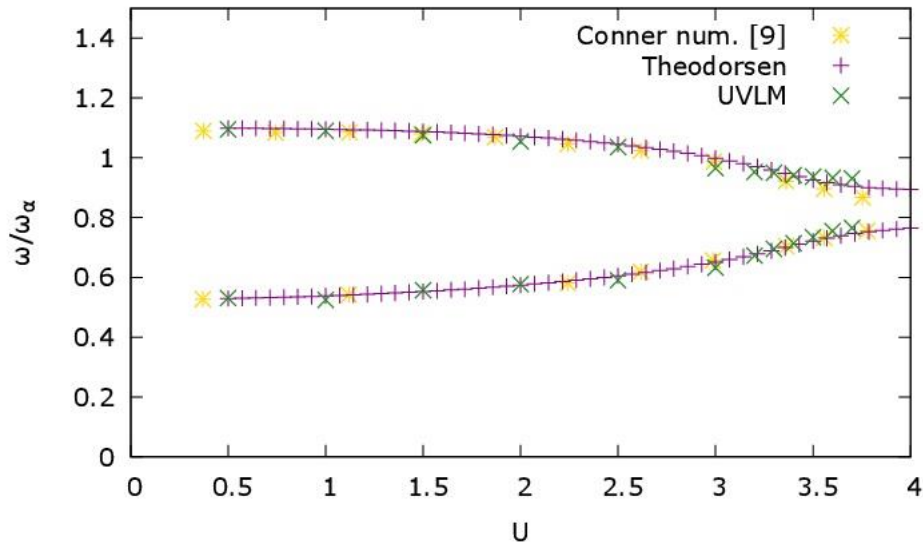


Figure 8. Dimensionless oscillation frequency against dimensionless wind speed for 3DOF linear case.

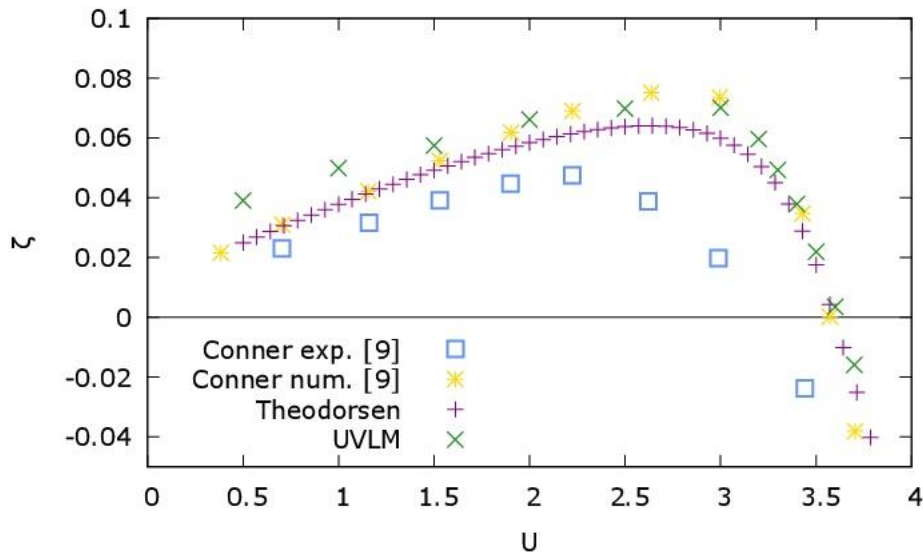


Figure 9. Damping against dimensionless wind speed for the 2DOF linear case.

	Theodorsen	UVLM	Conner Theo	Conner Exp.
V_f	3.57	3.61	3.57	3.08

Table 5. Comparison of linear flutter velocities for the 3DOF linear case.

Figures 6 to 9 show good agreement between Theodorsen and UVLM in capturing linear aeroelastic behaviour. These results have been compared with [8] for 2DOF and [9] for 3DOF. The values of the flutter speed are obtained, which are observed in the modal coalescence in the frequency diagrams and as the negative damping ratio in the damping diagrams, are given in table 4 for 2DOF and in table 5 for 3DOF case.

6. Non-Linear Aeroelasticity

For non-linear analysis, the same parameters shown in *table 3* are used. This time, cubic and freeplay non-linearities are introduced in the pitch DOF for the 2DOF case, and freeplay is introduced in the aileron deflection for the 3DOF case.

Below the linear flutter speed, U_f , both Theodorsen and UVLM succeeded in capturing the subcritical LCO and were compared with Zhao [8], Conner [9] and Kholodar [17]. Theodorsen captures the LCO but gives less accurate results probably due to the harmonic motion hypothesis.

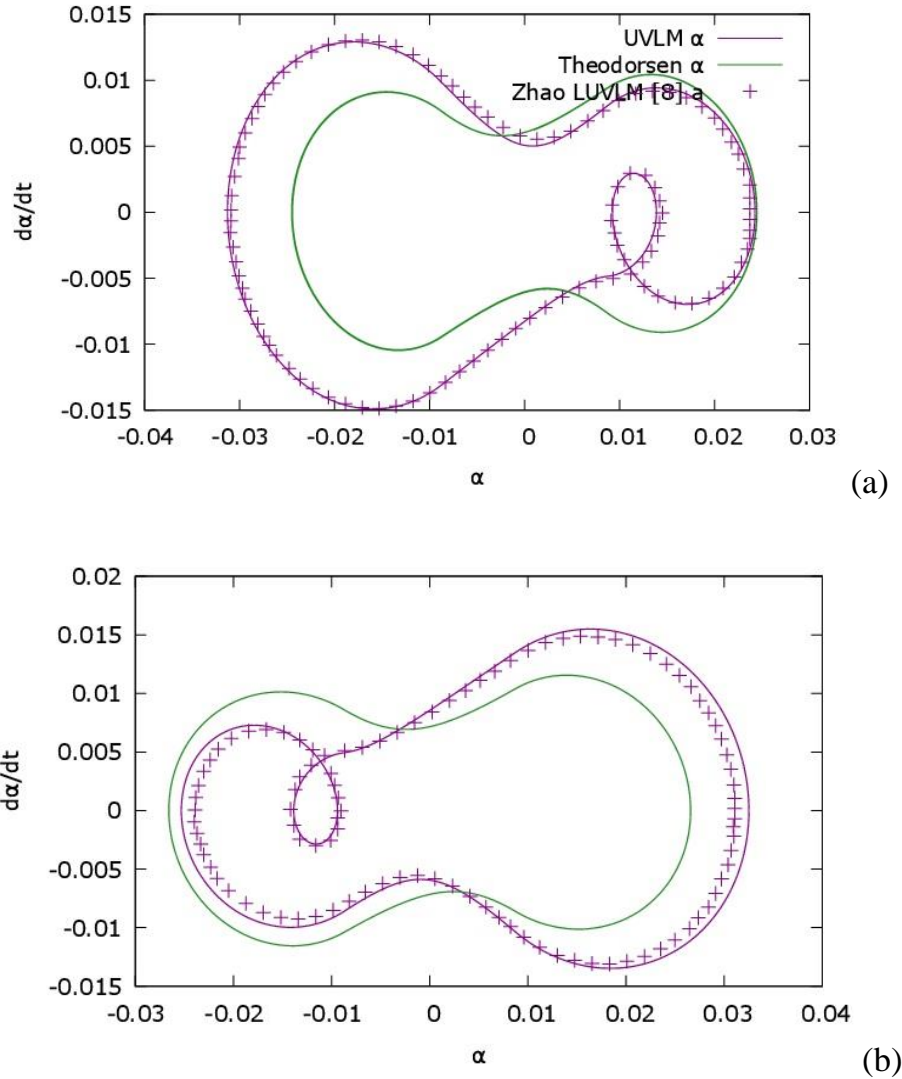


Figure 10. Change of phase trajectory of subcritical LCO. A) UVLM: $0.647U_f$, Theo.: $0.648U_f$, Zhao: $0.648U_f$. B) UVLM: $0.676U_f$, Theo.: $0.678U_f$, Zhao: $0.650U_f$.

Figure 10 (a) and (b) show an example of a symmetric change of phase trajectory with a small increase in amplitude during an LCO. This type of behaviour is observed several times throughout the subcritical regime once the system entered a LCO, in agreement with Zhao's [8] work.

For the 3 DOF non-linear case the root mean square (RMS) of each DOF's amplitude is calculated and divided by the freeplay gap in order to compare the results to those obtained by Conner, both numerically and experimentally [9], and numerically by Kholodar [17]. *Figure 9* shows the results as a function of speed divided by the linear flutter speed where: $(h, \alpha, \beta) = \frac{RMS(h, \alpha, \beta)}{2\beta_s}$.

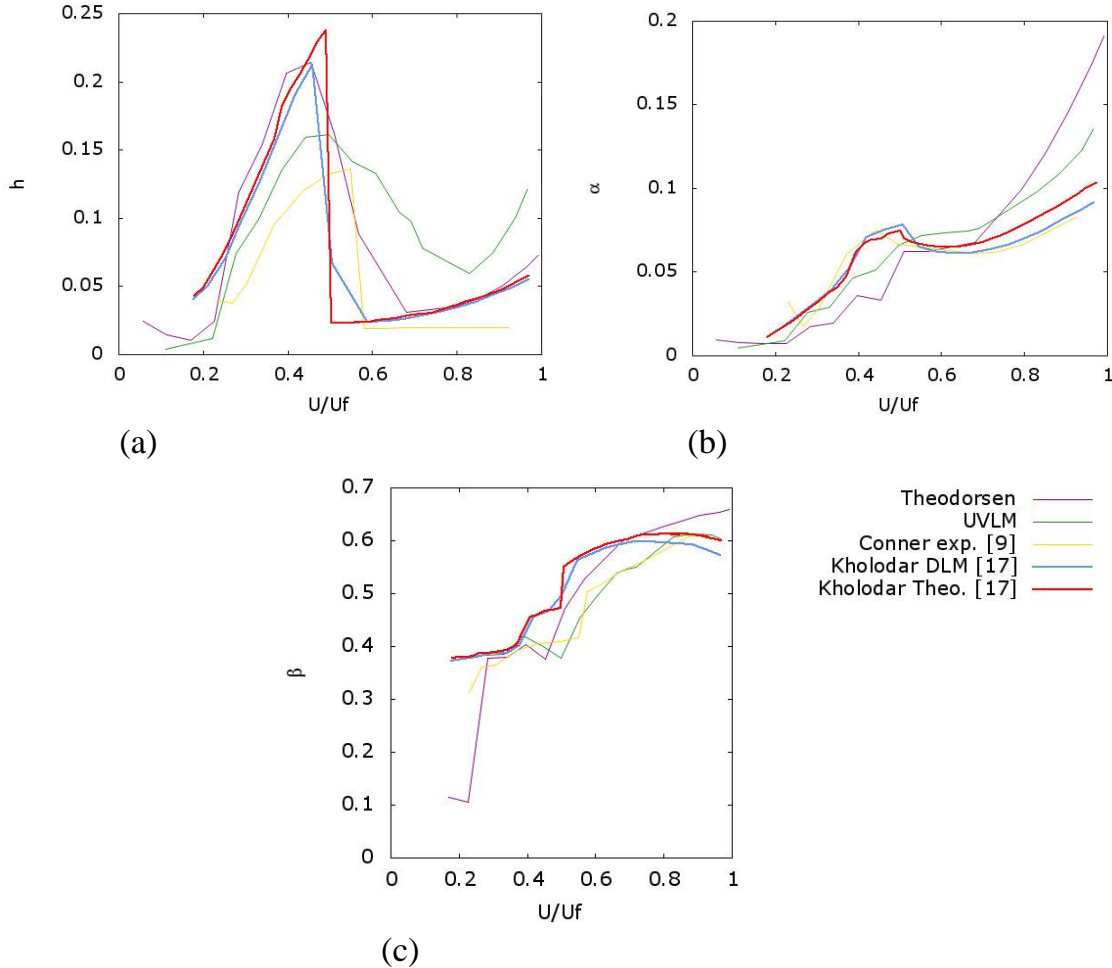


Figure 11. RMS amplitudes as a function of speed over linear flutter speed for (a) plunge DOF, (b) pitch DOF and (c) control surface deflection.

The subcritical LCOs present in the 3DOF system including freeplay are captured by the chosen methods as observed in *Figure 11*. For each DOF, motion amplitude varies as linear flutter speed fraction increases. Pitch angle and aileron deflection angle both increase with flow velocity; however, their respective rate of increase is different, as shown by all models. The heaving amplitude increases and then drops to lower amplitude LCO before increasing again as the velocity approaches linear flutter speed.

7. Conclusion

In this work, four methods are used to analyse unsteady aerodynamics and aeroelasticity of a 2D typical wing section: Theodorsen, UVLM, Euler and URANS. The structural model used is presented with a brief description of the methods used for aerodynamic force calculation. Once a mesh/time step validation is carried out, the unsteady aerodynamics low fidelity results have proven to match those obtained via Euler (medium fidelity) and URANS (high fidelity) approaches.

Regarding the aeroelastic analysis, the linear flutter speed is identified for a 2DOF and a 3DOF typical section. Non-linearities through freeplay and cubic stiffness in the pitching DOF for the 2DOF case and aileron freeplay for the 3DOF are added to the system to evaluate its response. Both Theodorsen and UVLM are able to capture subcritical LCOs similar to those identified in the literature.

Since they are low fidelity methods which include several simplifications, the computational time and cost of Theodorsen and UVLM are lower by several orders of magnitude than those of URANS or even Euler method. It has been shown that within a reasonable range, the results given by these low-fidelity methods are able to compete with higher fidelity methods giving very similar results and capturing the same types of phenomena.

References

1. F. Afonso, J. Vale, E. Oliveira, F. Lau, A. Suleman, *Non-linear aeroelastic response of high aspect-ratio wings in the frequency domain*. The Aeronautical Journal, 2017.
2. E. Breitbach, *Effects of structural non-linearities on aircraft vibration and flutter*. Tech. rep. DTIC Document, 1978.
3. A. Malher, *Amortisseurs passifs non linéaires pour le contrôle de l'instabilité de flottement*. PhD Thesis, Université de Paris-Saclay, 2016.
4. J. P. Thomas, E. H. Dowell, K. C. Hall, *Nonlinear Inviscid Aerodynamic Effects on Transonic Divergence, Flutter and Limit-Cycle Oscillations*. AIAA Journal, 2002.
5. R. L. Bisplinghoff, *Aeroelasticity*. Dover, 1996.
6. S. H. Strogatz, *Nonlinear Dynamics and Chaos with application in physics, biology, chemistry and engineering*. Addison-Wesley Publishing Company, 1994.
7. L. Amar, *Nonlinear passive control of an aeroelastic airfoil, simulations and Experimentations*. PhD Thesis, Toulouse University, 2017.
8. Y. Zhao, H. Hu, *Aeroelastic analysis of a non-linear airfoil based on unsteady vortex lattice model*. Journal of Sound and Vibration, 2004.
9. M. D. Conner, et al., *Nonlinear behavior of a typical airfoil section with control surface freeplay: a numerical and experimental study*. Journal of Fluids and Structures, 1997.
10. T. Theodorsen, *General theory of aerodynamic instability and mechanism of flutter*. National Advisory Committee for Aeronautics National Advisory Committee for Aeronautics, 1934.
11. S. L. Brunton, C. W. Rowley, *Empirical State-Space Representations for Theodorsen's Lift Model*. Journal of Fluids and Structures, 2012.
12. J. Katz, A. Plotkin, *Low-Speed Aerodynamics*. Cambridge University Press, 2001.
13. A. T. Levesque, A. Pigeon, T. Deloze, E. Laurendeau, *An overset grid 2D/Infinite swept wing URANS solver using Recursive Cartesian Virtual Grid method*. AIAA, 2015.
14. P. R. Spalart, S. R. Allmaras, *A one-equation turbulence model for aerodynamic flows*. 30th Aerospace Science Meeting and Exhibit, 1992.
15. S. Yang, S. Luo, and FengLiu, *Computation of the Flows over Flapping Airfoil by the Euler Equations*. AIAA, 2005.
16. R. J. S. Simpson, R. Palacios, *Numerical aspects of nonlinear flexible aircraft flight dynamics modeling*. AIAA, 2013.
17. B. D. Kholodar, *Nature of Freeplay-Induced Aeroelastic Oscillations*. Journal of Aircraft, 2013.